Study of d-electron correlations in skutterudite-related $Ce_3M_4Sn_{13}$ (M = Co, Ru, and Rh)

A. Ślebarski, J. Goraus, P. Witas, L. Kalinowski, and M. Fijałkowski
Institute of Physics, University of Silesia, 40-007 Katowice, Poland
(Received 30 September 2014; revised manuscript received 18 December 2014; published 5 January 2015)

We investigate the electronic structure of the skutterudite-related $Ce_3M_4Sn_{13}$ compounds, where metal M is Co, Ru, or Rh, using x-ray photoemission spectroscopy (XPS) and band structure calculations, both within local density approximation scheme and within scheme including additional Coulomb correlations (LDA+U). The d-electron states located near the Fermi level slightly change the intensity with applying the correlation energy U. We note the large impact of d-electron correlation, which is clearly observed in the change of Ce $5p$ states located about 18 eV in the valence band. Namely, for $Ce_3Rh_4Sn_{13}$ and $Ce_3Ru_4Sn_{13}$ the d-electron correlations significantly shift the $5p$ states towards higher binding energies, while for $Ce_3Co_4Sn_{13}$ the energy of the Ce $5p$ states almost does not depend on U. The influence of the d-electron correlations is also manifested by the positive magnetoresistivity (MR) of $Ce_3Rh_4Sn_{13}$ and the $Ce_{3-x}La_xRh_4Sn_{13}$ alloys that reaches 40% at the highest magnetic field ($B = 9$ T) for the sample $x = 0.6$, whereas only a small positive MR $\sim 0.5\%$ is observed in $Ce_3Ru_4Sn_{13}$. The magnetoresistivity of $Ce_3Co_4Sn_{13}$ exhibits quite different behavior and is negative.

DOI: 10.1103/PhysRevB.91.035101 PACS number(s): 71.27.+a, 72.15.Qm, 71.30.+h, 73.43.Qt

I. INTRODUCTION

Strongly correlated f- and d-electron systems are presently among the most intriguing and versatile materials, and their understanding represents one of the greatest challenges in condensed matter physics. A wide variety of interesting phenomena can be attributed to electronic correlations, among them metal-insulator transitions, heavy fermion and non-Fermi liquid behaviors, quantum criticality, and unconventional superconductivity. A key parameter in the strongly correlated electron systems (SCES) is the exchange between local magnetic moments of the f-electron states and the conduction carriers, J_{sf}. As J_{sf} is changed, the system can be tuned from a magnetically ordered metal to a heavy Fermi liquid under change in temperature, alloy composition, magnetic field, or pressure. When this transition occurs at the temperature $T = 0$ via change of tuning parameter, the transition is referred to as a quantum phase transition at a quantum critical point (QCP) [1]. Interestingly, as QCP is approached, the fluctuations between the two phases can result in a number of novel effects, such as unconventional superconductivity [2] and non-Fermi liquid (NFL) behaviors [3–5]. Recently [6–8], it was shown that the skutterudite-related $Ce_3M_4Sn_{13}$ heavy fermions exhibit a behavior characteristic of the Ce-based systems with comparable Kondo and magnetic energy scales, and can be near a magnetic QCP [9]. Within the system of $Ce_3M_4Sn_{13}$, $Ce_3Rh_4Sn_{13}$ has generated much interest due to positive magnetoresistivity (MR) effect, which has been recently suggested as a result of possible strong correlations originating from d electrons [10]. Our recent systematic studies of $Ce_3M_4Sn_{13}$ have shown that the MR effect depends on the metal M [10], in case of Co the MR is negative and $\sim$25% at the magnetic field of 9 T, while for Ru and Rh MR is positive and the maximal value of MR is $\sim$0.5% and 1% at $\sim$6 T, respectively, while for La-doped $Ce_3Ru_4Sn_{13}$ and $Ce_3Rh_4Sn_{13}$ samples MR is $\sim$35% and positive. Similarly, a strong positive MR was also experimentally confirmed for isostructural $Y_3Ir_4Ge_{13}$ [11] with nonmagnetic rare earth element, which suggest the d-electron contribution to abnormal MR behavior. It seems possible that the electronic structure of $Ce_3M_4Sn_{13}$-type materials, where M = Co, Ru, or Rh is d-electron type element, can be strongly influenced by the partially filled d orbitals, which have only a small direct overlap but still have itinerant character and provide strong d-electron correlations. There are known other examples of the systems with strong d-electron correlations documented experimentally; e.g., $Y_2Ir_2O_7$ described as a Mott insulator [12,13], FeSi [14], Fe_2TiSn [15], CeAgGa [16], and many others. In all cases the inclusion of Coulomb repulsion U on the transition metal d states gives satisfactory agreement between the calculated density of states and the XPS valence band spectra. Moreover, the correlation effect leads to heavy-Fermi-like behavior and formation of the insulating Kondo gap or pseudogap in FeSi and Fe_2TiSn, respectively. A very recent report on the studies of the spin-lattice relaxation rate in $YbFe_2Al_{10}$—the new class of *magnetic* Kondo insulators—has shown evidence for correlated $3d$ Fe moments strongly coupled via the conduction band, which hybridizes with Yb $4f$ states [17]. The results of these microscopic studies (NMR) are an important argument to consider the possible d-electron correlations coexisting with f-electron critical behaviors. In order to better depict properties of SCES apart from correlation already included within LDA scheme, additional term related to d or f electrons is included, then strongly correlated d or f electrons are better approximated using LDA+U. Introducing the on-site Coulomb repulsion $U \equiv U_d$ by LSDA+U we found that the calculated density of states (DOS) varies strongly with U for $Ce_3Rh_4Sn_{13}$, for $Ce_3Ru_4Sn_{13}$ the change is much smaller, while for $Ce_3Co_4Sn_{13}$ the effect of energy U on the energetic distribution of the DOSs is weak. We have also shown that in the case of $Ce_3Rh_4Sn_{13}$ the calculated electronic states at the binding energy of $\sim$18 eV are strongly U dependent and shift toward higher energy with increasing of U. For $Ce_3Ru_4Sn_{13}$ the effect is much weaker, while negligible in the case of $Ce_3Co_4Sn_{13}$. In order to estimate the electron correlation strength among d electrons, we compare the experimental XPS spectra at $\sim$18 eV (mostly attributed to Ce and Sn p states) with the *ab initio* results, where the calculations were carried out for different values of U. A comparison of the electronic structure

calculations and the XPS data gives distinct evidence for strong Coulomb correlation ($U \approx 6$ eV) among Rh $4d$ electrons; the effect is much weaker among Ru $4d$ states ($U \approx 3$–4 eV), while for the Co sample it is almost not observed [18]. We also analyze the chemical bondings between different atoms basing on the difference charge density maps, and show significant difference in charge distribution in $Ce_3Rh_4Sn_{13}$ and $Ce_3Ru_4Sn_{13}$. Here, $Ce_3Ru_4Sn_{13}$ with a very small MR effect is treated as a specific *reference* compound to $Ce_3Co_4Sn_{13}$ and $Ce_3Rh_4Sn_{13}$. We also present the difference charge density maps, specific heat, and susceptibility data for the La-doped $Ce_{3-x}La_xRu_4Sn_{13}$ to estimate the influence of f-electron contribution.

II. EXPERIMENTAL DETAILS

The band structure calculations were accomplished using fully relativistic full potential local orbital (FPLO) method (FPLO9-00-34 computer code [19]) within the local spin density approximation (LSDA). The exchange correlation potential V_{xc} was used in the form proposed by Perdew-Wang [20]. The number of k points in the irreducible wedge of Brillouin zone was 20 for each component of the series; due to a large volume of the unit cell this number was found sufficient to obtain well converged results. The spin-orbit interactions considered within fully relativistic calculations reduce symmetry of the magnetic unit cell depending on the chosen magnetization axis. In our calculations we used (0,0,1) as the chosen direction of the magnetization axis. Charge density was evaluated on a $52 \times 52 \times 52$ point grid within the unit cell.

The $Ce_3M_4Sn_{13}$ and $La_3M_4Sn_{13}$ samples ($M =$ Co, Rh, and Ru) were prepared by arc melting weighed amounts of each component. The dilute $Ce_{3-x}La_xRu_4Sn_{13}$ alloys were then prepared by diluting nominal compositions of the parent compounds. The samples were annealed at 870 °C for 2 weeks. All samples were carefully examined by x-ray diffraction analysis and found to be single phase with cubic structure (space group $Pm\bar{3}n$) [21]. Electrical resistivity ρ was investigated by a conventional four-point ac technique using a Quantum Design Physical Properties Measurement System (PPMS). Specific heat C was measured in the temperature range 0.4–300 K and in external magnetic fields up to 9 T using a Quantum Design PPMS platform. The dc magnetization M and magnetic susceptibility χ results were obtained using a commercial superconducting quantum interference device magnetometer from 1.8 K to 300 K in magnetic fields up to 7 T.

The XPS spectra were obtained with monochromatized Al K_α radiation at room temperature using a PHI 5700 ESCA spectrometer. The polycrystalline sample was broken under high vacuum better than 6×10^{-10} Torr immediately before taking a spectrum.

III. RESULTS AND DISCUSSION

A. Electronic structure; evidence for strong 5*d* electron correlations in $Ce_3Rh_4Sn_{13}$

The calculated densities of states (DOS) for the series of compounds $Ce_3Co_4Sn_{13}$, $Ce_3Ru_4Sn_{13}$, and $Ce_3Rh_4Sn_{13}$ are presented in Figs. 1–3, respectively. For comparison, the experimental XPS spectra are also shown. In the occupied part, there are three groups of features in the total DOSs. The energy range between 0 and −5 eV is dominated by the metal M d-electron states with a small contribution from $4f$ cerium states located near the Fermi level (the Ce $4f$ electrons form a narrow band with the center of gravity above the Fermi level). The energy range −6 to −10 eV is dominated by the Sn $5s$ states. The part of DOS located at about −17 eV is formed by the Ce $5p$ electrons. The electronic structures of the $Ce_3M_4Sn_{13}$ compounds were

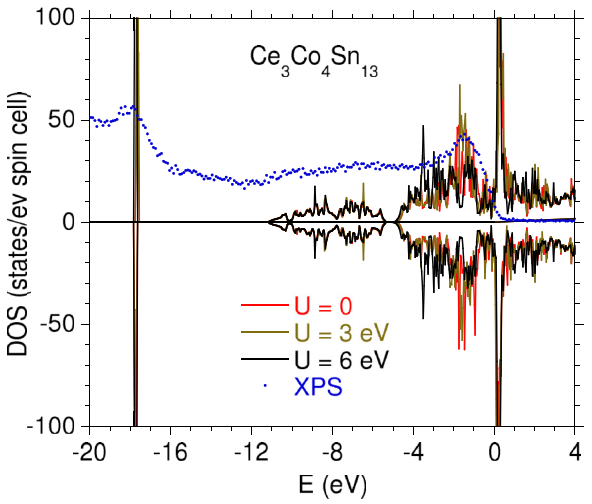

FIG. 1. (Color online) Valence band XPS spectrum for $Ce_3Co_4Sn_{13}$ compared with the calculated total and spin-resolve density of states within LSDA+U approximation. The TDOSs are calculated for energy $U_d = 0$, 3, and 6 eV, while the correlation energy between the $4f$ electrons $U_f = 0$. The maximum value of Ce $5p$ DOS is about 170 states/(eV spin cell).

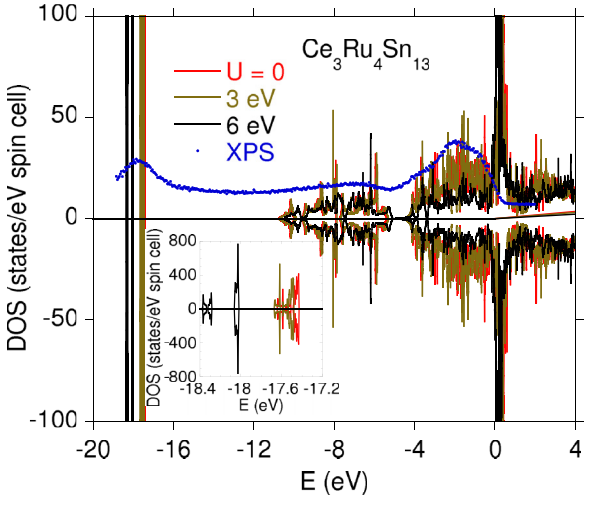

FIG. 2. (Color online) Valence band XPS spectrum for $Ce_3Ru_4Sn_{13}$ compared with the calculated total and spin-resolve density of states within LSDA+U approximation. The TDOSs are calculated for energy $U_d = 0$, 3, and 6 eV, with the correlation energy between the $4f$ electrons $U_f = 0$. The inset shows the calculated LSDA+U_d DOSs in the region of the $5p$ contribution.

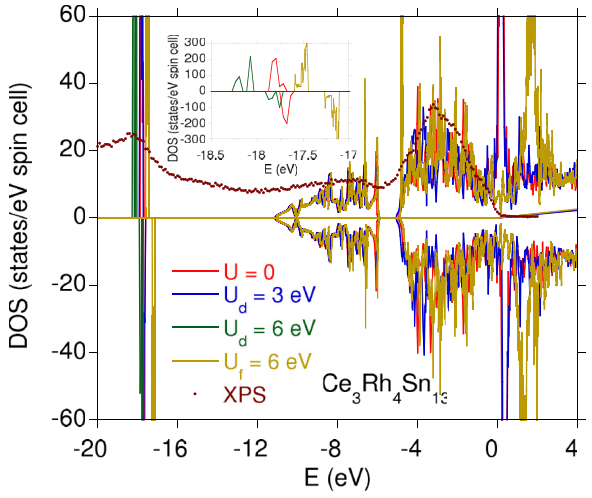

FIG. 3. (Color online) Valence band XPS spectrum for $Ce_3Rh_4Sn_{13}$ compared with the calculated total and spin-resolve density of states within LSDA+U approximation. The TDOSs are calculated for energy $U_d = 0$, 3, and 6 eV, with the correlation energy between the $4f$ electrons $U_f = 0$. The inset shows the calculated LSDA+U_d DOSs in the region of the $5p$ contribution.

recently discussed in the energy range between -10 eV and the Fermi level [8,22,23]; here we investigate the correlation induced effects in the bands. Figure 4 displays the valence band (VB) XPS spectra for the system of $Ce_{3-x}La_xCo_4Sn_{13}$ alloys to demonstrate that La doping does not change the nature of the bands [23] in parent $Ce_3M_4Sn_{13}$ compounds, but significantly changes the energy of the $5p$ electronic states. It should be noticed too that the LSDA+U Ce $5p$ states are strongly U dependent, especially if we take into account $d-d$ electron correlations. As will be discussed below, this change improves the consistency between the calculated and measured XPS spectra, hence justifying the LSDA+U approach. Figures 1–3 display a comparison of the calculated LSDA+U DOSs taking

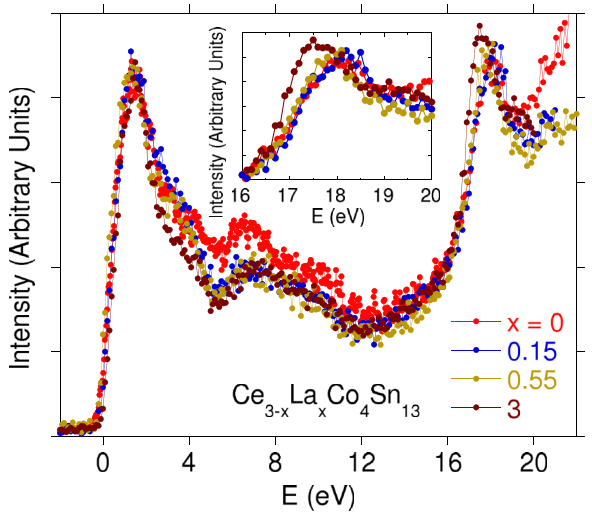

FIG. 4. (Color online) $Ce_{3-x}La_xCo_4Sn_{13}$; valence band XPS spectra, which show very similar structure. The location of Ce $5p$ electron states evidently depends on alloying (as shown in the inset).

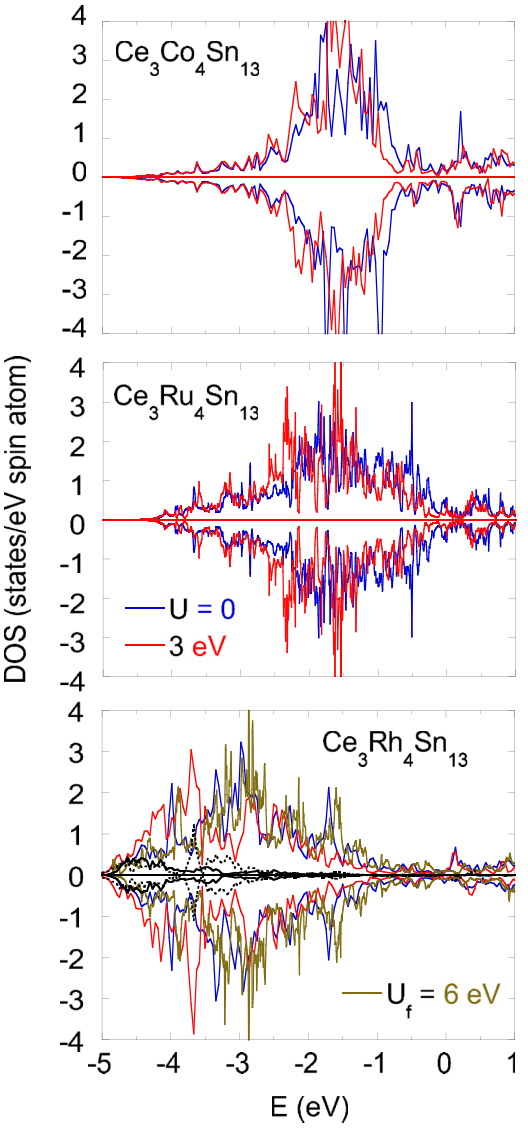

FIG. 5. (Color online) $3d$ (Co) or $4d$ (Ru, Rh) electron sta-tes for $Ce_3M_4Sn_{13}$, M = Co, Ru, and Rh, obtained from LSDA+U approaches, $U \equiv U_d = 0$ and 3 eV is the $d-d$ correlation energy, $U_f = 0$. The lowest panel also presents the LSDA+U d states calculated for $U_f = 6$ eV ($U_d = 0$). This panel also displays the Rh $4s$ states multiplied by the factor of 5, calculated for $U_d = 0$ (black solid line) and for $U_d = 3$ eV (black dotted line).

into account d-electron correlation $U_d = 0$, 3, and 6 eV, when the f-electron correlations are negligible ($U_f = 0$). The U_d effect is calculated weak for $Ce_3Co_4Sn_{13}$ (Fig. 1). Additional d-electron correlations lead to a small spectral weight transfer from ϵ_F to higher binding energies leading to an enhancement of intensity around 1.6 eV. For $Ce_3Ru_4Sn_{13}$ (Fig. 2) and $Ce_3Rh_4Sn_{13}$ (Fig. 3) the d-electron correlation effect gives slightly larger spectral weight transfer to lower binding energies and leads to enhancement of the total density of states around 1.6 eV for Ru and ~3.1 eV for Rh system. In Fig. 3 we also present the DOS within LSDA+U_f approach when $U_d = 0$; the effect of U on the energy of the maximum peak in DOS is negligible. In Fig. 5 we demonstrate the change of d-electron contributions with U. For $U_d \neq 0$, the

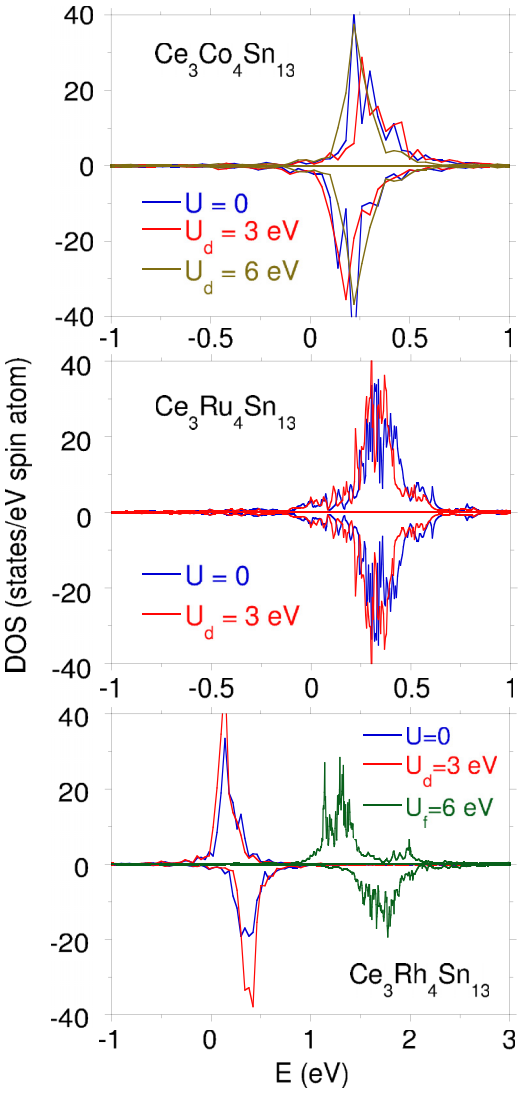

FIG. 6. (Color online) $4f$-electron states of $Ce_3M_4Sn_{13}$, M = Co, Ru, and Rh, obtained from LSDA+U approaches, $U \equiv U_d \neq 0$ is the $d-d$ correlation energy, $U_f = 0$. For $Ce_3Rh_4Sn_{13}$ we also present the partial DOSs calculated for $U_f = 6$ eV and $U_d = 0$.

metal M d-partial density of states slightly shifts towards higher binding energies with increase in intensity of the DOS maximum. Figure 5 also shows the $4s$ states of Rh, which are more hybridized with the $3d$ states for $U_d = 3$ eV than in the case of $U_d = 0$. It also is shown that the LSDA+U_f calculations change the electronic structure of the unoccupied f states (cf. Fig. 6), while the U_f effect on the d-band states is not significant. The Sn $5s$ and $5p$ states (not shown here) are practically not dependent on the change of U.

B. Chemical bonding in $Ce_3Ru_4Sn_{13}$

A large electronic specific heat coefficient, $C(T)/T$, of $Ce_3M_4Sn_{13}$, where M is Co [9], Rh [6], or Ru [8], suggested the quantum criticality and QCP in these compounds. In order to study the proximity of $Ce_3Co_4Sn_{13}$ and $Ce_3Rh_4Sn_{13}$ to the hypothetical QCP we recently investigated the physical properties of $Ce_{3-x}La_xM_4Sn_{13}$ and found that the substitution

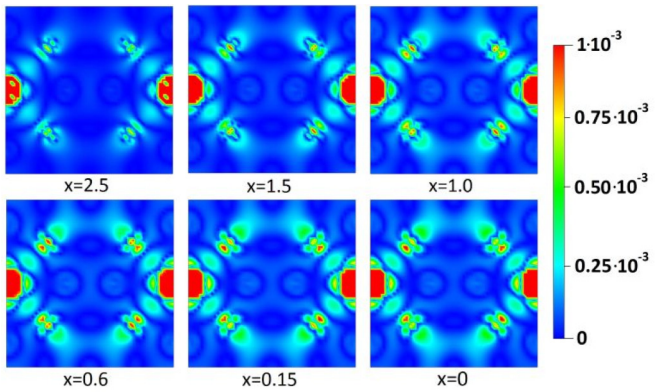

FIG. 7. (Color online) Difference charge densities $\Delta\rho_e$ (electron/Å^3) for the plane $(00\frac{1}{4})$ of $Ce_{3-x}La_xRu_4Sn_{13}$ provided with legend. The charge density maps reveal the strongest charge accumulations located between Rh and Sn2 atoms.

of Ce by larger La atom does not lead either to expected long range magnetic order or the QCP in La-doped $Ce_3Co_4Sn_{13}$ [24] and $Ce_3Rh_4Sn_{13}$ [10]. However, we found that these systems evolve from a magnetically correlated Kondo lattice state to a single-ion Kondo impurity state when the La content increases. Our recent study also established the $4f$ contribution to specific heat and magnetic susceptibility of the investigated systems in terms of the single-ion Kondo model. We now focus on the behavior of correlated d electrons in $Ce_3M_4Sn_{13}$. For this purpose we present here the charge density analysis around Ce, Ru, and Sn atoms when Ce is systematically substituted by La. Within the series of $Ce_3M_4Sn_{13}$, $Ce_3Ru_4Sn_{13}$ can be treated as a *reference compound* with very weak MR effect [$\Delta\rho/\rho(0)$ is $\sim$0.5% at the field $B = 2.5$ T, while with increasing of the field MR is negative for $B > 4.4$ T and $\sim -0.7\%$ at the highest magnetic field] in respect to larger and positive magnetoresistivity of $Ce_3Rh_4Sn_{13}$ for $B < 7$ T, or negative MR $\sim -25\%$ of $Ce_3Co_4Sn_{13}$ characteristic of the Kondo lattice. A particular positive to negative MR transition observed both in $Ce_3Ru_4Sn_{13}$ and $Ce_3Rh_4Sn_{13}$ and generated at low temperatures by the increasing magnetic field could be predominated by the nature of the $4f$ moments, conduction electrons, and the correlated and more localized d electrons of metal M; it will be discussed later in Sec. III C.

Figure 7 displays the 3D charge density map $\Delta\rho_e$ for different compounds of $Ce_{3-x}La_xRu_4Sn_{13}$ series obtained within virtual crystal approximation (VCA) in the plane $(00\frac{1}{4})$, displayed in Fig. 8. The charge density $\Delta\rho_e$ is defined as a difference between the electron density of the alloy x and the electron density of $La_3Ru_4Sn_{13}$. The charge density $\Delta\rho_e$ of $Ce_3Ru_4Sn_{13}$ exhibits strong charge accumulation between Ru and Sn2 atoms with the maximum in $\Delta\rho_e$ located near Ru atoms, which looks completely different than the $\Delta\rho_e$ distribution at Rh atoms in $Ce_3Rh_4Sn_{13}$ (cf. Ref. [10]). For clarity we present in Fig. 9 the change in charge density $\Delta\rho_e$ along the line representing the bonding between Sn1-Ru-Sn1 atoms.

The $\Delta\rho_e$ change on Ru is slightly positive and x dependent, and $\Delta\rho_e$ has a maximum value for $Ce_3Ru_4Sn_{13}$. It is worth noting that quite different behavior was observed for the $Ce_{3-x}La_xRh_4Sn_{13}$ system, where the opposite shift of the

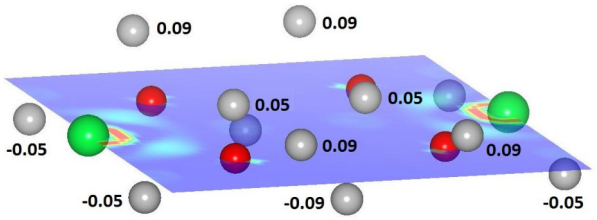

FIG. 8. (Color online) Plane $(00\frac{1}{4})$ with Ce (green balls), Ru (red), and Sn (gray) with the distance of each atom from the plane in respect to the lattice parameter. For temperatures lower than ∼160 K the site symmetry of the Ce atoms on the 6d crystallographic site is tetragonal [25]; here the local distortion of the Sn cage is not taken into account.

charge from the Rh atom to inside the Sn2 cage was calculated [10], and the change in difference charge density $\Delta\rho_e$ on Rh in $Ce_3Rh_4Sn_{13}$ was one order in magnitude stronger than that in $Ce_3Ru_4Sn_{13}$. Within the series of $Ce_3M_4Sn_{13}$ compounds, d orbitals of Rh atom in $Ce_3Rh_4Sn_{13}$ are the most tightly bound to the nucleus because of the largest occupation and the charge distribution $\Delta\rho_e$ near Rh atoms. In this case there is not so much overlap between the d orbitals and $d-d$ interactions become more important relative to $Ce_3Co_4Sn_{13}$ and $Ce_3Ru_4Sn_{13}$. Figures 10 and 11 show the variation in $\Delta\rho_e$ charge density of $Ce_{3-x}La_xRh_4Sn_{13}$ along the lines between the points (0,0,1/2) and (1/2,0,1/2) and between the atoms Sn1-Sn2, respectively. The observed bonding features among Ru and Sn2 atoms, as well as between Sn1 and Sn2 shown in Fig. 7 and Fig. 11, respectively, are characteristic of the $Ce_3M_4Sn_{13}$ cage-type compounds [10].

C. Magnetic properties of La-doped $Ce_3Ru_4Sn_{13}$

The magnetic results and core-level Ce 3d XPS spectra unambiguously corroborate in the $Ce_3M_4Sn_{13}$ compounds the stable configuration of the Ce 4f shell and rather weak hybridization Δ of the Ce 4f and conduction band states with

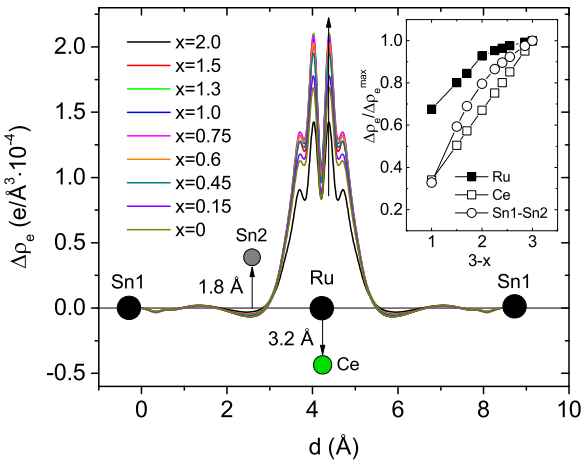

FIG. 9. (Color online) Charge density $\Delta\rho_e$ plotted along line representing the nearest-neighbor Sn1-Rh-Sn1 bonding. The inset displays the charge accumulation $\Delta\rho_e/\Delta\rho_e^{max}$ vs La doping, located on Ce, Rh atoms and in the middle of Sn1-Sn2 distance.

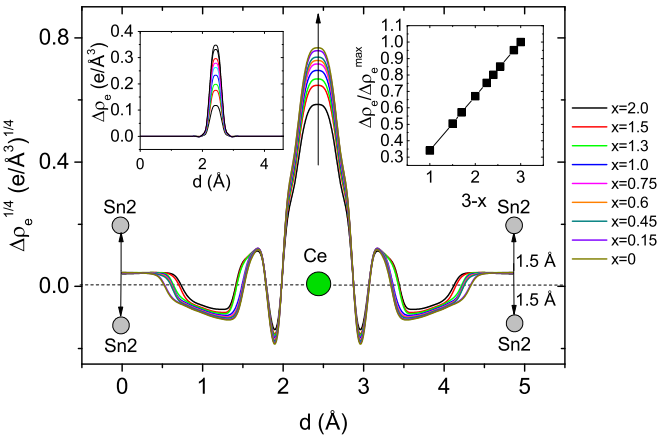

FIG. 10. (Color online) $Ce_{3-x}La_xRu_4Sn_{13}$; charge density $\Delta\rho_e^{1/4}$ near Ce. The left and right insets display the charge accumulation $\Delta\rho_e$ and $\Delta\rho_e/\Delta\rho_e^{max}$ on the rare-earth atom position 6d, respectively vs La doping; $\Delta\rho_e^{max}$ represents the maximum value of difference charge density obtained for $Ce_3Ru_4Sn_{13}$. The amplitude of the charge fluctuations is small; therefore, the figure exhibits $\Delta\rho_e^{1/4}$ to extend the effect.

$\Delta \approx 70$ meV [26]. Complex research indicates a single-ion Kondo behavior in these materials and the weak magnetic correlations as a result of the location of the magnetic moment on the rare earth [6,8,9]. Incomplete screening of Ce and, consequently, the magnetic correlation may arise from the charge transfer in the bond between Ce and Sn atoms (cf. Fig 10). On the other hand, the covalent bonding between Ru (metal M) and Sn2 atoms leads to deformation of the Sn_{12} cages, which is reflected in the crystalline-electric field (CEF) susceptibility χ [in Fig. 12(a)]. The $\chi(T)$ and $1/\chi(T)$ can be well fitted by the Van Vleck formula [27], $\chi_{CEF} = \frac{N\mu_B^2}{k_B}\frac{\sum_i(\frac{a_i}{T}+b_i)e^{-\beta\Delta_i}}{\sum_i g_i e^{-\beta\Delta_i}} + \chi_0$, considering the tetragonal Ce point symmetry of Ce^{3+} ion

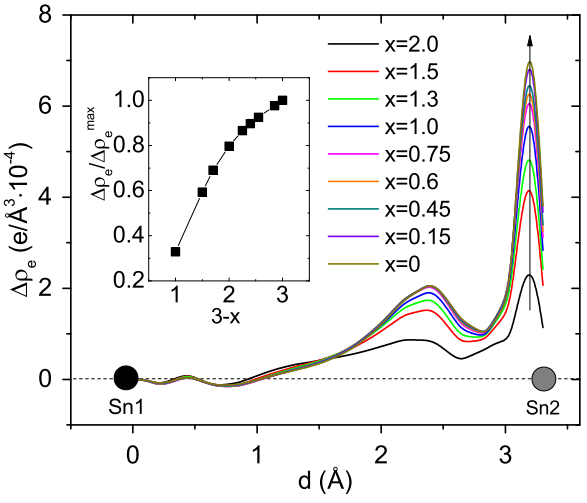

FIG. 11. (Color online) $Ce_{3-x}La_xRu_4Sn_{13}$; charge density $\Delta\rho_e$ plotted on the line connecting Sn1 and Sn2 atoms. The inset displays the charge accumulation $\Delta\rho_e$ and $\Delta\rho_e/\Delta\rho_e^{max}$ located between Sn1 and Sn2 vs La doping; $\Delta\rho_e^{max}$ represents the maximum value of difference charge density obtained for $Ce_3Ru_4Sn_{13}$.

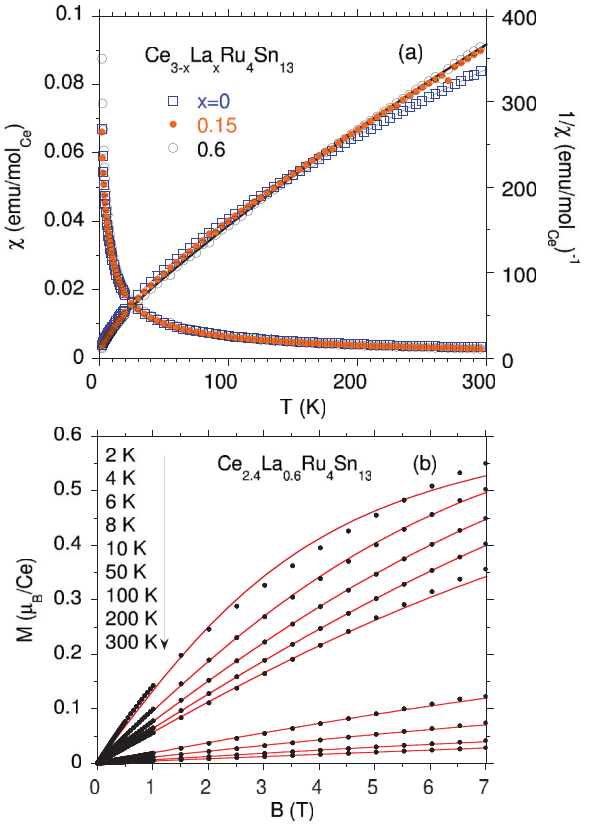

FIG. 12. (Color online) (a) Magnetic susceptibility χ and $1/\chi$ of $Ce_{3-x}La_xRu_4Sn_{13}$ in external field of 1000 Gs. The line represents the CEF fit to $1/\chi$ data with the two excited doublets separated from the ground state doublet by energy $\Delta_1 \approx 10$ K and $\Delta_2 \approx 150$ K, respectively. Panel (b) displays magnetization M vs magnetic field and the fit of the Langevin function to the experimental data.

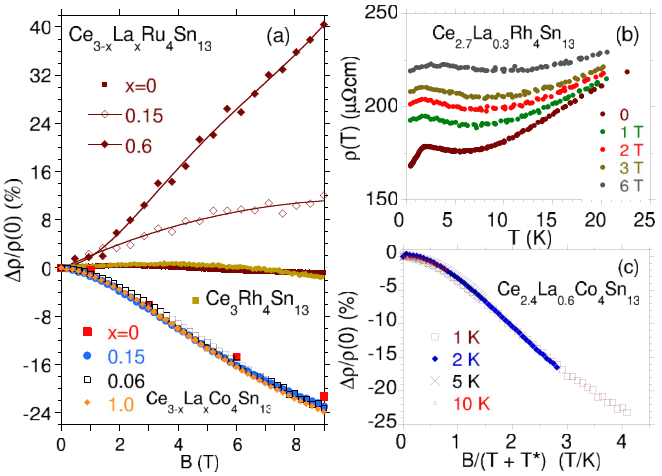

FIG. 13. (Color online) (a) Magnetoresistivity $\Delta\rho/\rho(0)$ at $T = 1$ K vs magnetic field, $\Delta\rho = \rho(B) - \rho(0)$. Panel (b) displays resistivity $\rho(T)$ for $Ce_{2.7}La_{0.3}Ru_4Sn_{13}$ at different magnetic fields. Panel (c) shows $\Delta\rho/\rho(0)$ vs $B/(T + T^*)$.

which splits into three doublets separated from the ground state by energies $\Delta_1 \approx 10$ K and $\Delta_2 \approx 150$ K, respectively, and $\chi_0 \sim 5 \times 10^{-4}$–$2 \times 10^{-3}$ emu/mol. Within the series of $Ce_3M_4Sn_{13}$ compounds we noted quite different splitting of the $J = 5/2$ multiplet in $Ce_3Ru_4Sn_{13}$ than the respective crystal field level scheme of $Ce_3Rh_4Sn_{13}$ and $Ce_3Co_4Sn_{13}$. For both letter compounds the CEF splitting obtained from the magnetic susceptibility and specific heat data agrees well with an inelastic neutron scattering experiment [25] ($\Delta_1 \approx 90$ K; $\Delta_2 \approx 350$ K [23]). Quite large χ_0 may signal d-electron correlation effect. There is also another argument for strong d-electron correlations, namely, the magnetic susceptibilities of the $Ce_{3-x}La_xRu_4Sn_{13}$ compounds shown in Fig. 12(a) appear to scale well with the content of Ce. This behavior gives evidence for single-ion Kondo behavior when La content increases. This observation also speaks in favor of the role of d-electron correlations, as opposed to inter- or intra-atomic Ce correlations which would otherwise be expected to dominate the character of the electronic properties at the Fermi level. Within the series of $Ce_3M_4Sn_{13}$, also the electronic specific-heat coefficient $\gamma_0 \equiv C(T)/T$, obtained from the linear dependence of $C(T)/T = \gamma_0 + \beta T^2$ is ~350 mJ/K^{2}mol for $Ce_3Rh_4Sn_{13}$, while for $Ce_3Co_4Sn_{13}$ $\gamma_0 \approx 200$ mJ/K^{2}mol, which again gives support for d-electron correlations much stronger in the Rh sample than in $Ce_3Co_4Sn_{13}$.

The magnetization $M(B)$ isotherms are for the all components x well approximated by the Langevin function $L(y) = \coth(y) - 1/y$, where $y = \mu B/k_BT$ and are similar, which well confirm the paramagnetism of the $Ce_{3-x}La_xRu_4Sn_{13}$ system. Small discrepancy between the experimental and calculated $M(H)$ for the isotherm at $T = 2$ K can be explained by the presence of short-range magnetic correlations. In Fig. 12(b) we show the magnetization M vs magnetic field isotherms for $Ce_{2.4}La_{0.6}Ru_4Sn_{13}$, as an example.

Recently, we noted [24] that the MR data confirm a conventional Kondo character for $Ce_3Co_4Sn_{13}$. In a magnetic field the Kondo scattering of the conduction electrons is partially quenched, leading to a negative magnetoresistance. This behavior is essentially caused by the progressive freezing out of spin flip scattering due to the aligning of the Kondo impurity spin along the magnetic field. Figure 13(a) shows negative magnetoresistance MR $\equiv \Delta\rho/\rho(0)$ for selected compounds $Ce_{1-x}La_xCo_4Sn_{13}$, which when are replotted as a function of $B/(T + T^\star)$ [28] give scaling with $T^\star \approx 1.2$ K [24], where $T^\star$ is a characteristic single impurity temperature related to Kondo temperature [cf. Fig. 13(c)]. In Fig. 13(a) the magnetoresistance isotherms, however, exhibit quite different behavior either for $Ce_3Ru_4Sn_{13}$ or $Ce_3Rh_4Sn_{13}$, namely MR of the both samples is positive (MR_{max} is ~0.5% or ~1%, respectively) at the magnetic fields $H <$ ~4.5 T and $H <\sim$ 7 T, respectively, and change sign from positive to negative at higher magnetic fields. A similar positive magnetoresistance and its field dependence; e.g., in $CeCu_6$ [29], appears at the Kondo temperature T_K, and has been pointed out due to the gap structure of the Kondo resonance slightly above the Fermi level [30]. In case of $Ce_3Ru_4Sn_{13}$ and $Ce_3Rh_4Sn_{13}$ we indeed calculated within LSDA+U and with $U_f \neq 0$ or $U_d \neq 0$ a pseudogap at about 0.04 eV above the Fermi level in the total DOS. However, the positive MR is also observed for the both compounds at $T \gg T_K$ [31] [cf. Fig. 13(b)], which suggests different mechanism of the positive MR in $Ce_3Ru_4Sn_{13}$, $Ce_3Rh_4Sn_{13}$, and their La-doped alloys. The positive MR effect in $Ce_3Rh_4Sn_{13}$ and $Ce_3Ru_4Sn_{13}$ is strongly enhanced by

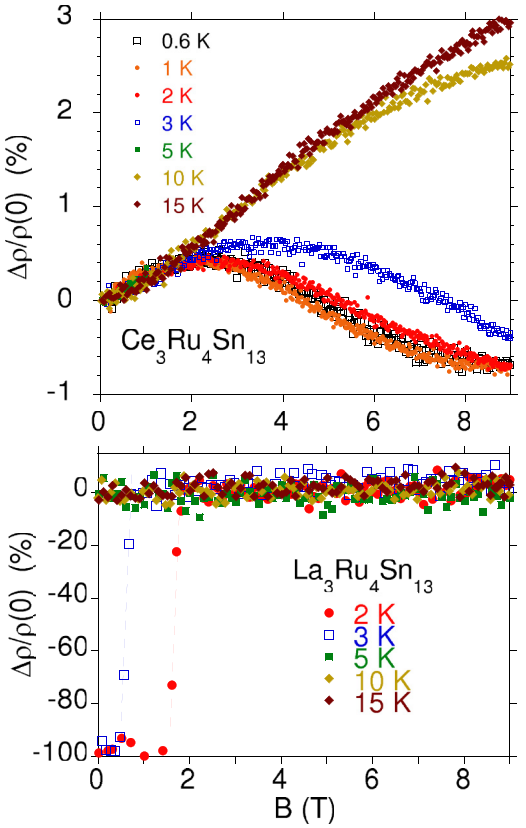

FIG. 14. (Color online) Magnetoresistivity $\Delta\rho/\rho(0)$ at different temperatures vs magnetic field. Upper panel displays resistivity MR for $Ce_3Ru_4Sn_{13}$. The lower panel compares zero MR effect in $La_3Ru_4Sn_{13}$; the rapid change of magnetoresistivity at $T = 2$ K and 3 K is due to the superconducting state.

dilution of a nonmagnetic La ion [cf. Fig. 13(a)]. Considering that in the series of $Ce_{1-x}La_xM_4Sn_{13}$ nearly 2/3 of the conduction band character is constituted by the conduction band electrons of Sn atoms, one expects a significant free-electron character of the electrons participating in electric transport process, and for which a positive magnetoresistivity is supposed. To confirm this thesis we measured the MR of the pair of compounds: $Ce_3M_4Sn_{13}$ and $La_3M_4Sn_{13}$, respectively, at the same temperatures. The MR data for $Ce_3Ru_4Sn_{13}$ and $La_3Ru_4Sn_{13}$ compared in Fig. 14 do not confirm this hypothesis. The same result was observed for the pair of compounds $Ce_3Rh_4Sn_{13}$ and $La_3Rh_4Sn_{13}$, again with almost zero MR effect in La counterpart. Considering that the negative MR in $Ce_3Co_4Sn_{13}$ and its La-doped alloys has a conventional Kondo character, we conclude that the positive magnetoresistivity in $Ce_3Ru_4Sn_{13}$ and $Ce_3Rh_4Sn_{13}$ can result from the d-electron correlations (for $La_3Co_4Sn_{13}$ counterpart we measured MR $\cong 0$ at different temperatures; the result is the same as that shown in the lower panel of Fig. 14).

D. Discussion

Although the electron correlation effects are explicitly manifested in the large energy scale, namely the LSDA+U calculations explained the change of binding energy of the Ce $5p$ electronic states, well documented experimentally by XPS, various thermodynamic properties are essentially determined by the correlated electronic states near the Fermi energy ϵ_F ($|\epsilon - \epsilon_F| \approx k_BT$). Some strongly correlated materials display a great sensitivity to changes of the resistivity in an applied magnetic field (e.g., colossal magnetoresistance). In La-doped $Ce_3Rh_4Sn_{13}$ we observed strong and positive magnetoresistence effect below ~50 K. This positive magnetoresistence behavior cannot be described well by any of the theoretical models proposed for f-electron metals. Positive and large MR of $Ce_3Rh_4Sn_{13}$ is different than the expected negative MR predicted by Moriya and Kawabata [32] for systems with ferromagnetic fluctuations. In the case of antiferromagnetic fluctuations, external magnetic field enhances the fluctuations, giving a positive rise to MR, whereas fluctuation with ferromagnetic origin usually are suppressed by magnetic field and the MR is negative. Positive MR is typical of classic non-Fermi liquid systems and the effect was found for $CeCu_2Si_2$, $CeNi_2Ge_2$ [33], or $U_{0.9}Th_{0.1}Be_{13}$ [34]; all systems are closed to QCP, where applied field suppresses antiferromagnetic fluctuations. This is, however, not a case either of $Ce_3Rh_4Sn_{13}$ or similar $Ce_3M_4Sn_{13}$ materials, for which the QCP has not been experimentally obtained [9,10,24]. Moreover, the low-temperature specific heat C/T data gives evidence for the similar magnetic correlations in all the investigated $Ce_3M_4Sn_{13}$ compounds, where $M =$ Co, Ru, and Rh [35]. We try to explain the observation of a field induced positive magnetoresistivity in $Ce_3Ru_4Sn_{13}$ and $Ce_3Rh_4Sn_{13}$ on the base of the strong interaction effects in a d-electron transition metal. Previously, Strydom [11] observed similar positive MR effect in nonmagnetic $Y_3Ir_4Ge_{13}$ and proposed that Coulomb interaction effects can dominate the field-dependent electronic transport in this material. He suggested that strong interaction effects in d-electron Ir metal could be brought about by a large d band spectral weight of the conduction electrons, while the d-band character of conduction electrons could result from a presence of these states at the Fermi level, or alternatively from a strong $s - d$ hybridization. We suppose that the both effects are important here. Our former Fermi surface analysis has shown for other cage-type compounds $LaRh_2Sn_4$ [36] and $LaRhSn_2$ [37] a parallel section of the sheets of d-electron type origin, which could generate instabilities and be responsible for the spin fluctuation effects. The spin fluctuations were observed too for the $La_3M_4Sn_{13}$ compounds [24,38] as a possible reason of Fermi surface nesting. Indeed, for metals mean-field theories predict that spin fluctuations induced by applied magnetic field produce a positive MR effect in antiferromagnets [39]. However, the most intriguing results from resistivity measurement, i.e., the existence of both positive and negative MR values, complicates the interpretation (similar MR vs B behavior, but much stronger was recently reported for GdSi single crystal [40], where the peculiar MR positive MR value to negative MR value transition was discussed as a result of coexistence of the $4f$ moments and the polaronic $5d$ carriers). The second effect, hybridization between the $s - d$ electron state, is visible in the LSDA+U band structure calculations; cf. Fig. 5. In order to deeper understand the f- and d-electron correlations and their impact on the low-temperature physical properties

of the $La_3M_4Sn_{13}$ and $Ce_3M_4Sn_{13}$ materials, where M is the d-electron element, we suggest an infrared optical study to obtain a spectral weight transfer.

Finally, in the context of strong electron correlations we discuss the calculated DOSs of $La_3Co_4Sn_{13}$ in connection with the apparent disparity between results of the higher spin lattice relaxation rate (SLR) [41] and electronic specific heat coefficient [42] values, compared to the slightly lower DOS value for $Ce_3Co_4Sn_{13}$. First, the Co partial density of d-states value at the Fermi level in $La_3Co_4Sn_{13}$ is ∼0.6 states/(eV Co), while the DOS value of 1.2 states/(eV Co) was found in SLR rate studies. Such a discrepancy of the DOS values can be interpreted in the nonmagnetic compound as evidence of d-electron correlations. A similar conclusion results from a specific heat coefficient study. For $La_3Co_4Sn_{13}$ the calculated DOS value at ϵ_F is ∼9.7 states/(eV f.u.), while $\gamma = \frac{\pi^2}{3} k_B N(\epsilon_F)$ gives enhanced DOS value of ∼11.5 states/(eV f.u.), which can result from correlations. Secondly, the DFT calculations give for $Ce_3Co_4Sn_{13}$ the Co partial density of d states ∼0.4 states/(eV Co); i.e., slightly smaller value than the $N(\epsilon_F)$ obtained for the non-4f counterpart, while DOS at the Fermi level estimated from the electronic specific heat coefficient ∼80 states/(eV f.u.) is much larger than the calculated $N(\epsilon_F) \approx 10$ states/(eV f.u.). We suggest that weak, however, present d-electron correlations in $Ce_3Co_4Sn_{13}$ could be responsible for the formation of the pseudogap near the Fermi level (note FeSi [14] or Fe_2TiSn [15] are known d-electron Kondo insulators with characteristic gap or pseudogap in DOS at the Fermi level) and thereby for the small value of the calculated DOS, while the f-electron correlations and magnetic instability (magnetic correlations) dominate the experimental value of DOS in $Ce_3Co_4Sn_{13}$.

IV. CONCLUSIONS

We studied the electronic structure of $Ce_3M_4Sn_{13}$, where M is Co, Ru, or Rh. A comparison of the electronic structure calculations and the XPS data gives evidence for strong Coulomb correlation among metal M d-electron states. We argue that the positive magnetoresistivity in $Ce_3Rh_4Sn_{13}$ and in La-doped $Ce_3Rh_4Sn_{13}$ and $Ce_3Ru_4Sn_{13}$ alloys can be interpreted as an effect of strong d-electron correlations. In the past few years, the number of intermetallic compounds based on rare earth and transition metals and having coexistence of f- and d-electron correlations increases. Our investigations clearly corroborate such a complex behavior in $Ce_3M_4Sn_{13}$ materials, where M = Ru and Rh. The observed behavior in magnetoresistivity is of a Kondo-ion behavior in the case of $Ce_3Co_4Sn_{13}$, whereas MR evidences the presence of d-electron correlations among transition metal M in $Ce_3Ru_4Sn_{13}$ and $Ce_3Rh_4Sn_{13}$. These results are consistent with the band structure calculations and XPS data, which evidently show in $Ce_3Ru_4Sn_{13}$ and $Ce_3Rh_4Sn_{13}$ the shift of the location of the Ce 5p states towards higher binding energies and reconstruction of metal M d bands near the Fermi level.

ACKNOWLEDGMENT

We thank National Science Centre (NCN) for financial support, on the basis of decision No. DEC-2012/07/B/ST3/03027.

[1] There are also known examples [e.g., $YbAlB_4$, S. Nakatsuji, K. Kuga, Y. Machida, T. Tayama, T. Sakakibara, Y. Karaki, H. Ishimoto, S. Yonezawa, Y. Maeno, E. Pearson, G. G. Lonzarich, L. Balicas, H. Lee, and Z. Fisk, Nat. Phys. **4**, 603 (2008)] in which QCP appears to occur accidentally; i.e., without external tuning.

[2] F. Steglich, J. Aarts, C. D. Bredl, W. Lieke, D. Meschede, W. Franz, and H. Schäfer, Phys. Rev. Lett. **43**, 1892 (1979).

[3] J. A. Hertz, Phys. Rev. B **14**, 1165 (1976).

[4] A. J. Millis, Phys. Rev. B **48**, 7183 (1993).

[5] T. Moriya and T. Takimoto, J. Phys. Soc. Jpn. **64**, 960 (1995).

[6] U. Köhler, A. P. Pikul, N. Oeschler, T. Westerkamp, A. M. Strydom, and F. Steglich, J. Phys.: Condens. Matter **19**, 386207 (2007).

[7] E. L. Thomas, H.-O. Lee, A. N. Bonkston, S. MaQuilon, P. Klavins, M. Moldovan, D. P. Young, Z. Fisk, and J. Y. Chan, J. Solid State Chem. **179**, 1642 (2006).

[8] A. Ślebarski, M. Fijałkowski, J. Goraus, L. Kalinowski, and P. Witas, J. Alloys Compds. **615**, 921 (2014).

[9] A. L. Cornelius, A. D. Christianson, J. L. Lawrence, V. Fritsch, E. D. Bauer, J. L. Sarrao, J. D. Thompson, and P. G. Pagliuso, Physica B **378-380**, 113 (2006).

[10] A. Ślebarski, P. Witas, J. Goraus, L. Kalinowski, and M. Fijałkowski, Phys. Rev. B **90**, 075123 (2014).

[11] A. M. Strydom, J. Phys.: Condens. Matter **19**, 386205 (2007).

[12] D. Yanagishima and Y. Maeno, J. Phys. Soc. Jpn. **70**, 2880 (2001).

[13] R. S. Singh, V. R. R. Medicherla, K. Maiti, and E. V. Sampathkumaran, Phys. Rev. B **77**, 201102 (2008).

[14] J. F. DiTusa, K. Friemelt, E. Bucher, G. Aeppli, and A. P. Ramirez, Phys. Rev. B **58**, 10288 (1998).

[15] A. Ślebarski, M. B. Maple, E. J. Freeman, C. Sirvent, D. Tworuszka, M. Orzechowska, A. Wrona, A. Jezierski, S. Chiuzbaian, and M. Neumann, Phys. Rev. B **62**, 3296 (2000).

[16] J. Goraus, A. Ślebarski, and M. Fijałkowski, Phys. Status Solidi B **248**, 2857 (2011).

[17] P. Khuntia, P. Peratheepan, A. M. Strydom, Y. Utsumi, K.-T. Ko, K.-D. Tsuei, L. H. Tjeng, F. Steglich, and M. Baenitz, Phys. Rev. Lett. **113**, 216403 (2014).

[18] For Co, Ru the d-electron shell is occupied by the number of electrons $n = 7$, while for Rh, n is 8. The correlation energy is n dependent.

[19] K. Koepernik and H. Eschrig, Phys. Rev. B **59**, 1743 (1999); I. Opahle, K. Koepernik, and H. Eschrig, *ibid.* **60**, 14035 (1999); K. Koepernik, B. Velicky, R. Hayn, and H. Eschrig, *ibid.* **55**, 5717 (1997); H. Eschrig, K. Koepernik, and I. Chaplygin, J. Solid State Chem. **176**, 482 (2003); www.fplo.de

[20] J. P. Perdew and Y. Wang, Phys. Rev. B **45**, 13244 (1992).

[21] J. P. Remeika, G. P. Espinosa, A. S. Cooper, H. Barz, J. M. Rowel, D. B. McWhan, J. M. Vandenberg, D. E. Moncton, Z. Fizk, L. D. Woolf, H. C. Hamaker, M. B. Maple, G. Shirane,

and W. Thomlinson, Solid State Commun. **34**, 923 (1980); J. L. Hodeau, M. Marezio, J. P. Remeika, and C. H. Chen, *ibid.* **42**, 97 (1982).
[22] G. Zhong, X. Lei, and J. Mao, Phys. Rev. B **79**, 094424 (2009).
[23] M. Gamża, W. Schnelle, A. Ślebarski, U. Burkhardt, R. Gumeniuk, and H. Rosner, J. Phys.: Condens. Matter **20**, 395208 (2008).
[24] A. Ślebarski, M. Fijałkowski, and J. Goraus, Intermetallics **54**, 199 (2014).
[25] D. T. Adroja, A. M. Strydom, A. P. Murani, W. A. Kockelmann, and A. Fraile, Physica B **403**, 898 (2008).
[26] A. Ślebarski and J. Goraus, Phys. Rev. B **88**, 155122 (2013).
[27] J. Mulak, J. Less Common Met. **121**, 141 (1986).
[28] P. Schlottmann, Phys. Rep. **181**, 1 (1989).
[29] A. Sumiyama, Y. Oda, H. Nagano, Y. Onuki, K. Shibutani, and T. Komatsubara, J. Phys. Soc. Jpn. **55**, 1294 (1986).
[30] N. Kawakami and A. Okiji, J. Phys. Soc. Jpn. **55**, 2114 (1986).
[31] The Kondo temperature $T_K \approx 1.5$ K obtained for $Ce_3M_4Sn_{13}$, $M =$ Co, Rh, and Ru, decreases with La doping in the system of $Ce_{3-x}La_xM_4Sn_{13}$ alloys; cf. Refs. [10,24].
[32] T. Moriya and A. Kawabata, J. Phys. Soc. Jpn. **34**, 639 (1973).
[33] F. Steglich, P. Hellmann, S. Thomas, P. Gegenwart, A. Link, R. Helfrich, G. Sparn, M. Lang, C. Geibel, and W. Assums, Physica B **237-238**, 192 (1997).
[34] R. P. Dickey, M. C. de Andrade, J. Herrmann, M. B. Maple, F. G. Aliev, and R. Villar, Phys. Rev. B **56**, 11169 (1997).
[35] The specific heat data for 9 T field displays a broad peak at ∼3 K in the $C(T)$ and $C(T)/T$ of all $Ce_3M_4Sn_{13}$ compounds, which show the characteristic features of a Schottky anomaly. This anomaly can be caused by excitations between Zeeman levels of the ground crystal electric field doublet (cf. Ref. [25]). However, below 3 K the $C(T)/T$ data show a behavior characteristic of heavy Fermi liquid with an increasing C/T when $T \to 0$ and its large value of about 4 J/K^2mol_{Ce} expected for $T = 0$ (cf. Refs. [8,10]).
[36] M. Gamża, W. Schnelle, R. Gumeniuk, Yu. Prots, A. Ślebarski, H. Rosner, and Yu. Grin, J. Phys.: Condens. Matter **21**, 325601 (2009).
[37] M. Gamża, A. Ślebarski, and H. Rosner, J. Phys.: Condens. Matter **20**, 025201 (2008).
[38] C. S. Lue, H. F. Liu, S.-L. Hsu, M. W. Chu, H. Y. Liao, and Y. K. Kuo, Phys. Rev. B **85**, 205120 (2012).
[39] H. Yamada and S. Takada, J. Phys. Soc. Jpn. **34**, 51 (1973).
[40] H. Li, Y. Xiao, B. Schmitz, J. Persson, W. Schmidt, P. Meuffels, G. Roth, and T. Brückel, Sci. Rep. **2**, 750 (2012).
[41] H. F. Liu, C. N. Kuo, C. S. Lue, K.-Z. Syu, and Y. K. Kuo, Phys. Rev. B **88**, 115113 (2013).
[42] A. Ślebarski, M. Fijałkowski, M. M. Maśka, M. Mierzejewski, B. D. White, and M. B. Maple, Phys. Rev. B **89**, 125111 (2014).